

# Design of Short High-Power $TE_{11}$ – $HE_{11}$ Mode Converters in Highly Overmoded Corrugated Waveguides

Manfred Thumm, Annemarie Jacobs, and Mario Sorolla Ayza, *Member, IEEE*

**Abstract**—A theoretical parametric study of  $TE_{11}$  to  $HE_{11}$  mode conversion in highly oversized, circumferentially corrugated circular waveguides with different inner diameters is presented for various frequencies in the range of 28 to 140 GHz. The depth of the annular slots is tapered gradually from one half to one quarter wavelength. Computer-aided optimization of converter length, shape of corrugations, and nonlinear slot depth variation has been achieved with a scattering matrix code employing the modal field matching techniques (modular analysis concept). Relatively short mode transducers with matched converter lengths of  $L \approx \pi / \Delta\beta_{[TE_{11}-TM_{11}]}$  are feasible. In all cases the  $HE_{11}$  output mode purity is 99% to 99.5%. The maximum cross-polarization and input-reflection levels are below  $-29$  dB and  $-50$  dB, respectively. Experimental results at 70 GHz (I.D. = 27.79 mm) are in excellent agreement with the theoretically predicted performance.

## I. INTRODUCTION

THE balanced  $HE_{11}$  mode propagating in an overmoded, circumferentially corrugated waveguide is in many respects ideal for a variety of applications of high-power millimeter waves, for example deep-space millimeter-wave radar and communication as well as electron cyclotron resonance heating (ECRH) of magnetically confined thermonuclear fusion plasmas with high-power gyrotron oscillators [1], [2]. Radiated from an open-ended waveguide antenna (or scalar feed horn), this hybrid mode exhibits desirable radiation characteristics such as almost perfect linear polarization with very low cross-polarization and an axisymmetric narrow pencil beam containing about 98% of the radiated power with very low side-lobe levels [3]. It couples excellently to the fundamental Gaussian free-space mode for quasi-optical propagation through reflector beam waveguides. Furthermore, the  $HE_{11}$  mode is particularly suited for low-loss, high-power transmission through highly overmoded tubular waveguides since its ohmic attenuation is lower than that of any other mode [3]. This “Gaussian-like” mode can be generated from  $TE_{0n}$  gyrotron output modes via the two

three-step mode conversion sequences

$$TE_{0n} \rightarrow TE_{01} \rightarrow TE_{11} \rightarrow HE_{11} [2]$$

$$TE_{0n} \rightarrow TE_{01} \rightarrow TM_{11} \rightarrow HE_{11} [1].$$

The first scheme, which uses the  $TE_{11}$  mode as polarized intermediate mode, has the advantage that all converters can be made without bends. This allows an arbitrary choice and fast change of the polarization plane by simply rotating the  $TE_{01}$  to  $TE_{11}$  converter around its axis. In addition, there is no danger of  $EH_{11}$  surface mode generation, as is the case for  $TM_{11}$  to  $HE_{11}$  conversion.

Adiabatic  $TE_{11}$  to  $HE_{11}$  mode conversion is achieved in a straight, circumferentially corrugated waveguide section whose slot depth is gradually tapered from an initial value of about  $\lambda/2$  to a final value of approximately  $\lambda/4$ , where  $\lambda$  is the free-space wavelength. The generation of free-space Gaussian beams with such corrugated mode transducers is well known in areas such as radio astronomy, radar, and modern terrestrial and satellite communication, where optimized corrugated horns (scalar feeds) are used as prime focus feeds in high-performance, low-noise reflector antenna systems [3]. Conversion of  $TE_{11}$  to  $HE_{11}$  in corrugated circular waveguides with slowly varying depth of the annular slots has been investigated theoretically using the surface impedance formalism [4], [5] or the scattering matrix formalism [6]–[10] for relatively small ratios  $D/\lambda$ , where  $D$  is the waveguide diameter. In the present case of high-power mode converters the waveguide diameter,  $D$ , must be much larger than a wavelength,  $\lambda$ . In such highly oversized multimode waveguides with changing corrugation, the varying slot depth allows coupling to many other higher order hybrid mode branches with identical azimuthal mode index  $m=1$ . The transducer length and the nonlinear slot depth profile have to be optimized in order to achieve a high conversion efficiency to the desired mode [11], [12].

This work reports a systematic scattering matrix code analysis of  $TE_{11}$  to  $HE_{11}$  mode conversion in highly oversized corrugated waveguides for various frequencies in the range from 28 to 140 GHz with  $ka$  values from 11.7 to 40.8, where  $k = 2\pi/\lambda$  is the free-space propagation constant and  $a$  the waveguide radius. Cyclic mode beating and phasing effects allow relatively short mode transducers with high efficiency. Scaling formulas are deduced which allow an intuitive and phenomenological approach to the design of these compo-

Manuscript received March 26, 1990; revised August 15, 1990.

M. Thumm was with the Institut für Plasmaforschung, Universität Stuttgart, D-7000 Stuttgart 80, Germany. He is now with the Institut für Hochstfrequenztechnik und Elektronik, Universität Karlsruhe, D-7500 Karlsruhe 1, Germany.

A. Jacobs is with the Institut für Plasmaforschung, Universität Stuttgart, D-7000 Stuttgart 80, Germany.

M. Sorolla Ayza was with the Institut für Plasmaforschung, Universität Stuttgart, D-7000 Stuttgart 80, Germany. He is now with Mier Comunicaciones, S.A., Placa De L'ajuntament, 2, 08520 Les Franqueses Del Vallès, Barcelona, Spain.

IEEE Log Number 9041092.

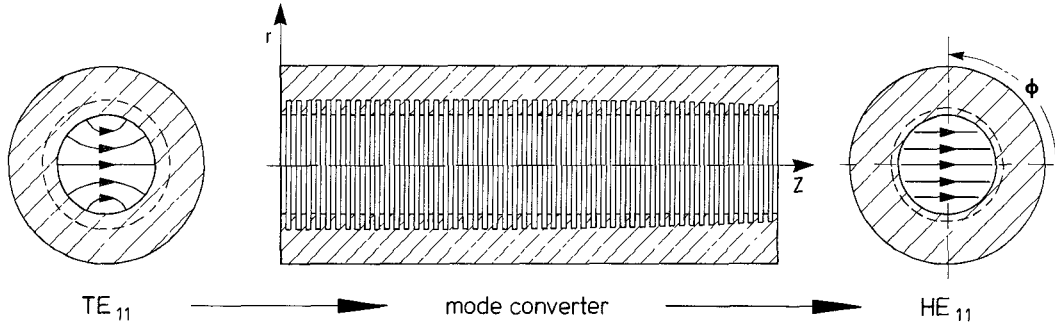


Fig. 1. Principle of the TE<sub>11</sub> to HE<sub>11</sub> mode converter (cross-sectional view) and polar coordinate system ( $r, \phi, z$ ).

nents. Experimental data are reported for short and long 70 GHz TE<sub>11</sub> to HE<sub>11</sub> mode transducers with  $D = 27.79$  mm ( $ka = 20.39$ ).

## II. GENERAL CONSIDERATIONS

In cases where the waveguide diameter  $D = 2a$  becomes fairly large compared to the free-space wavelength  $\lambda$ , and when the period  $p$  of the annular slots is assumed small compared with the guide wavelength, no space harmonics need to be considered and a circumferentially corrugated waveguide wall may be modeled well by an effective anisotropic surface reactance (wall impedance concept: WIC) where the circumferential component is zero ( $Z_\phi = 0$ ) and the longitudinal component is finite:  $Z_z = jZ_0Z$  (coordinate system, see Fig. 1). Here  $Z$  is a normalized reactance and  $Z_0 = \sqrt{\mu_0/\epsilon_0}$  is the impedance of free space. For  $ka \gg 1$  the surface reactance  $Z$  may well be approximated as [13]

$$Z = \frac{w}{p} \cdot \frac{\tan(k \cdot d)}{1 + \frac{\tan(k \cdot d)}{2ka}} \quad (1)$$

where  $d$  and  $w$  are the mechanical slot depth and width, respectively, and  $p$  is the corrugation period. The factor  $w/p$  reflects the fact that the finite width of the corrugation teeth reduces the reactance, while the  $\tan(kd)$  dependence indicates that the annular slots act like short-circuited transmission lines. The longitudinal surface reactance may be reduced further if the slots and teeth are rounded [3].

The propagation behavior of HE<sub>mn</sub> and EH<sub>mn</sub> hybrid modes ( $m > 0$ ) is described by the characteristic or dispersion equation for the roots  $X_{mn} = K_{mn} \cdot a$  [3], [5]:

$$\frac{1}{Zka} = \frac{1}{X_{mn}^2} \frac{J_m(X_{mn})}{X_{mn} J'_m(X_{mn})} \left[ \frac{m^2 \beta_{mn}^2}{k^2} - \left( \frac{X_{mn} J'_m(X_{mn})}{J_m(X_{mn})} \right)^2 \right] \quad (2)$$

where  $K_{mn}$  is the radial separation constant (transverse wavenumber),  $\beta_{mn} = (k^2 - K_{mn}^2)^{1/2}$  is the longitudinal propagation constant in the waveguide; and  $J_m(X)$  is a Bessel function of the first kind and order  $m$ .

TE<sub>0n</sub> modes are not affected by the corrugation. The numerical solution of the characteristic equation (2) for a corrugated waveguide with  $2a = 27.79$  mm at  $f = 70$  GHz is plotted in Fig. 2. The eigenvalues  $K_{mn} \cdot a$  of normal HE<sub>mn</sub> and EH<sub>mn</sub> hybrid modes are monotonically varying functions of the relative slot depth  $d/(\lambda/4)$ . For  $d/(\lambda/4) = 0, 2, 4, \dots$

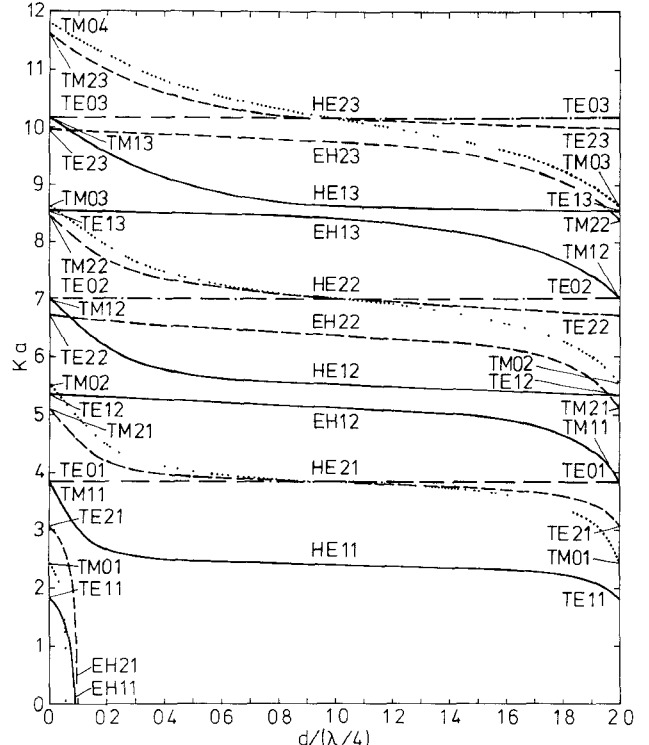


Fig. 2. Eigenvalues  $X_{mn}$  of the characteristic equation versus normalized electrical slot depth  $d/(\lambda/4)$  for various modes in a circumferentially corrugated waveguide with inner radius  $a = 13.9$  mm at 70 GHz ( $ka = 20.39$ ).

( $Z = 0$ ) the eigenvalues of hybrid modes are equal to the eigenvalues of the modes of a smooth waveguide (it is assumed that there are no ohmic losses in the waveguide). Hybrid modes consist of linear combinations of TE<sub>mn</sub> and TM<sub>mn</sub> field components which are determined by the hybrid factor [3]:

$$\bar{\Lambda}_{mn} = - \frac{J_m(X_{mn})}{X_{mn} J'_m(X_{mn})}. \quad (3)$$

The balanced hybrid condition  $(\bar{\Lambda})^2 = 1$  (at  $d/(\lambda/4) = 1, 3, 5, \dots$  with  $Z = \infty$ ) has the two roots

$$\bar{\Lambda} = +1 \quad (4)$$

corresponding to HE modes and

$$\bar{\Lambda} = -1 \quad (5)$$

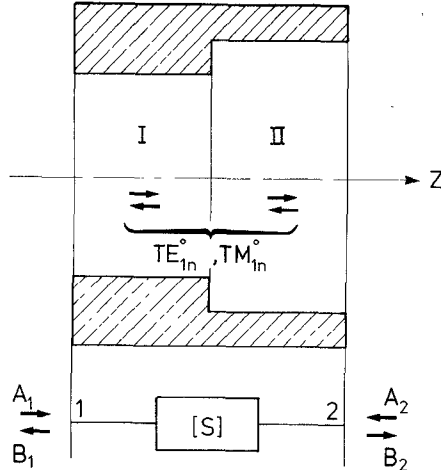


Fig. 3. Basic module used to determine the electromagnetic field by mode matching analysis inside the corrugated mode converter of Fig. 1.

corresponding to EH modes. Any waveguide possessing a diameter  $D \gg \lambda$  and a wall with high surface reactance can propagate such a hybrid mode (corrugated, dielectric-coated metal, and dielectric waveguides [13], [14]). Here  $|\bar{\Lambda}| = \infty$  corresponds to TE modes and  $\bar{\Lambda} = 0$  to TM modes.

Adiabatic TE<sub>11</sub> to HE<sub>11</sub> mode conversion is achieved in a straight corrugated waveguide section in which the electrical depth (effective depth) of the slots decreases slowly from an initial value of  $\lambda/2$  to a final slot depth of approximately  $\lambda/4$  (see Fig. 1). The longitudinal surface reactance inside the waveguide is capacitively decreasing from zero at the smooth-walled input waveguide (the input slot appearing as a short circuit) to the high value required in the converter output.

The varying slot depth allows coupling only to higher order modes with identical azimuthal mode number [7], [11], and unwanted mode conversion is associated primarily with the nearby TM<sub>11</sub> to EH<sub>12</sub> branch. The EH<sub>12</sub> hybrid mode has a radiation pattern which is entirely cross-polarized in the 45° plane. If excited it degrades seriously the cross-polarization performance of the transducer output. Therefore the converter must be long enough to suppress the excitation of this unwanted spurious mode.

### III. MODULAR ANALYSIS CONCEPT (MAC)

Computer-aided optimization of the required converter length, of the period and shape of corrugations, and of the nonlinear slot depth variation has been achieved with a scattering matrix code employing the modal field expansion techniques [9] in order to get a pure HE<sub>11</sub> output mode [11], [12]. In this approach the inner part of the mode transducer is decomposed into a certain number of modules. Each consists of an abrupt junction of two circular waveguides of different diameters (regions I and II, see Fig. 3). The radial slots are modeled by connecting two such modules in cascade, with the larger waveguides facing each other.

If the converter is excited by the fundamental TE<sub>11</sub> mode in the smooth-walled feeding waveguide, the complete set of eigenfunctions is represented by the corresponding forward- and backward-traveling cylindrical waveguide TE<sub>1n</sub> and TM<sub>1n</sub> modes, which can be excited at each radius discontinuity (circular symmetry:  $\Delta m = 0$ ). The boundary conditions for

the tangential electric and magnetic fields across the common interfaces between the subregions lead to an infinite system of coupled linear equations for the unknown expansion coefficients, which in matrix form [9] reads

$$\begin{aligned} [M_0][B_2] &= [M_1][A_1] + [M_2][A_2], \\ [B_1] &= [A_1] + [M_3][A_2] + [M_4][B_2]. \end{aligned} \quad (6)$$

The vectors  $[A_1]$  and  $[A_2]$  contain the complex amplitudes of the incident TE<sub>1n</sub> and TM<sub>1n</sub> modes in regions I and II, respectively, whereas  $[B_1]$  and  $[B_2]$  denote the amplitudes of the corresponding reflected modes. The matrices  $[M_i]$  ( $i = 0, 1, \dots, 4$ ) depend on the geometrical parameters of the module and on the wavelength. Their dimensions are infinite and therefore have to be truncated for the numerical analysis, which comprises the inversion of the quadratic matrix  $[M_0]$  and some matrix multiplications to arrive at the scattering matrix [9]

$$\begin{pmatrix} [B_1] \\ [B_2] \end{pmatrix} = \begin{pmatrix} [S_{11}][S_{12}] \\ [S_{21}][S_{22}] \end{pmatrix} \begin{pmatrix} [A_1] \\ [A_2] \end{pmatrix} \quad (7)$$

of the individual corrugation module. In order to achieve satisfactory convergence, the number of propagating and evanescent TE<sub>1n</sub>/TM<sub>1n</sub> modes that have to be taken into account in the circular waveguide sections amounts to about ten times the ratio of the waveguide radius to the wavelength. The number of modes which can propagate in the individual sections depends on that ratio and, hence, varies from slot to slot along the converter wall. Even in highly overmoded waveguides, the propagation behavior of modes close to cutoff is influenced to some extent by the resistivity of the waveguide wall. Finite conductivity is included in the computer code to model the performance of the transducer accurately.

The scattering matrix of the complete mode transformer valid for reference planes located at the input and the output can be determined by cascading module by module via the corresponding scattering matrices following an iterative algorithm [9]. This procedure is somewhat cumbersome to evaluate, but the exclusive use of scattering matrices has the advantage over other network representations of avoiding numerical problems associated with the inversion of ill-conditioned matrices originating from the necessity of including evanescent modes in the analysis.

The modular analysis concept outlined above has the advantage of incorporating all geometrical parameters of the mode converter and does not impose any restrictions on their values as the surface impedance description. From the cascaded overall scattering matrix the input reflection and the distribution of the electromagnetic field (amplitudes and phases of the different eigenmodes), i.e., the mode content at the output of the transformer, can be calculated. In order to check the accuracy of the calculations and the mode purity by far-field radiation pattern measurements, copolar (E-plane, H-plane, 45°-plane) and cross-polar (45°-plane) patterns radiated at the output of the converter are computed.

### IV. COMPUTATIONAL RESULTS

The numerical calculations have been performed on a CRAY-II computer, typical CPU times being between 10 and 30 min per run. First preparatory computations revealed

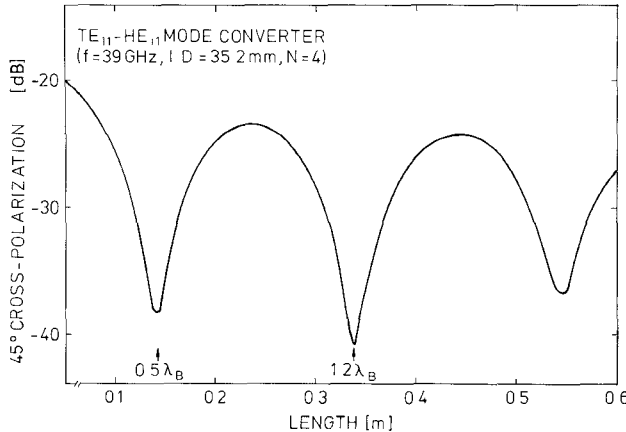


Fig. 4. Computed peak level of the cross-polar power in the 45° plane of the far-field pattern radiated from the output of a 39 GHz TE<sub>11</sub> to HE<sub>11</sub> mode converter ( $D = 35.2$  mm,  $N = 4$ ) versus converter length. Vertical axis is dB.

an optimum choice of the corrugation profile for the different mode transducers (eight different  $ka$  values) with respect to mechanical feasibility and mode conversion performance, namely period  $p = \lambda/3$ , the slot width  $w$  being half the corrugation period (slot width  $\equiv$  tooth width  $= \lambda/6$ ). In order to reduce the length of the mode transformer, the depth of the annular slots has to be tapered nonlinearly, with the slowest decrease near the converter input, where the coupling coefficient for hopping to the EH<sub>12</sub> branch is largest [4]. In all cases the slot depth profile was chosen to be parabolic, following an  $N$ -power law:

$$d(z) = (\lambda/2) - (\lambda/4)(z/L)^N \quad (8)$$

where  $N$  depends on the  $ka$  value of the mode transducer and  $L$  is the converter length.

The reference design data for the mode converters require that the mode purity be 99%. Here the mode purity is defined as the sum of the relative powers in the modes TE<sub>11</sub> and TM<sub>11</sub>, with compositions between 82% TE<sub>11</sub>/17% TM<sub>11</sub> and 87% TE<sub>11</sub>/12% TM<sub>11</sub> and a phase difference of approximately 180°. This results in a symmetrical far-field radiation pattern, with side-lobe level  $\lesssim -25$  dB, maximum cross-polarization  $\lesssim -30$  dB, and input reflection  $\lesssim -50$  dB.

Figs. 4, 5, and 6 show for  $ka = 14.39$  ( $f = 39$  GHz,  $D = 35.2$  mm,  $N = 4$ ) the predicted peak level of the cross-polar power in the 45°-plane, the fractional power in the TE<sub>11</sub> and TM<sub>11</sub> components, and their phase difference versus the length of the mode converter. These numerical results reveal that owing to cyclic mode beating and phasing effects several solutions exist which are characterized by the desired design data for the mode transducers. Relatively short TE<sub>11</sub> to HE<sub>11</sub> mode transformers are feasible.

The optimum conversion lengths are

$$L_1 \approx 0.5 \cdot \lambda_B \text{ (short converter)}$$

$$L_2 \approx 1.2 \cdot \lambda_B \text{ (long converter)}$$

where  $\lambda_B$  is the beat wavelength of the TE<sub>11</sub> and TM<sub>11</sub> components in the corresponding smooth-walled circular waveguide. The predicted performances of short and long mode transducers are practically identical. In both cases the

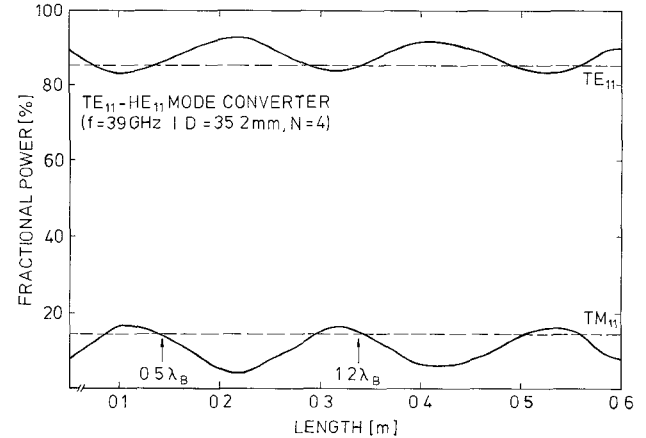


Fig. 5. Computed fractional power in the TE<sub>11</sub> and TM<sub>11</sub> cylindrical waveguide eigenmodes at the output of a 39 GHz TE<sub>11</sub> to HE<sub>11</sub> mode converter ( $D = 35.2$  mm,  $N = 4$ ) versus converter length. Vertical axis gives percentage.

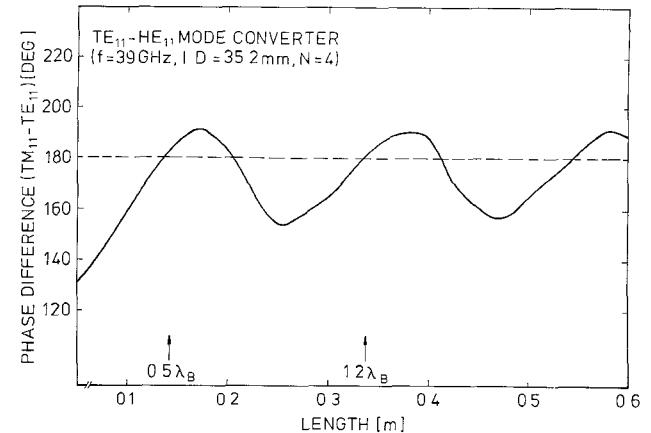


Fig. 6. Computed relative phase of the TE<sub>11</sub> and TM<sub>11</sub> cylindrical waveguide eigenmodes at the output of a 39 GHz TE<sub>11</sub> to HE<sub>11</sub> mode converter ( $D = 35.2$  mm,  $N = 4$ ) versus converter length.

theoretical bandwidth is 5 GHz (maximum 45° cross-polarization lower than -25 dB), which is by far sufficient since high-power gyrotron oscillators are narrow-band devices. No ring-loaded radial slots have to be introduced.

The computed peak level of the 45° cross-polarization achievable with strictly linear ( $N = 1$ ) or with parabolic (different orders  $N$ ) profile tapering versus the converter length in the case of  $ka = 13.05$  ( $f = 28$  GHz,  $D = 44.45$  mm) is plotted in Fig. 7. Variation of  $N$  leads to approximately the same values of the cross-polarization if the cross-polarization is large and to minimum value of the cross-polar level at the optimum transducer lengths but does not change the optimum conversion lengths.

The calculations show that the optimum  $N$  number of the parabolic slot depth profile has to be increased from  $N = 4$  at  $ka = 12$  to approximately  $N \gtrsim 30$  for  $ka = 40$ . This means that the optimum profile is very close to that of constant coupling along the converter which was used in the surface-impedance concept description of a 60 GHz TM<sub>11</sub> to HE<sub>11</sub> mode transformer [1]. The coupling coefficient  $c(d)$  for branch hopping from TE<sub>11</sub>-HE<sub>11</sub> to TM<sub>11</sub>-EH<sub>12</sub> caused by

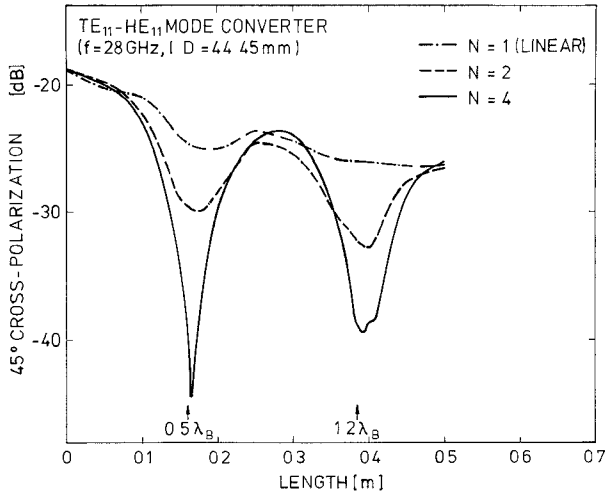


Fig. 7. Computed peak level of the cross-polar power in the 45° plane of the far-field pattern radiated from the output of 28 GHz TE<sub>11</sub> to HE<sub>11</sub> mode converters ( $D = 44.45$  mm) versus converter length for linear ( $N = 1$ ) and parabolic ( $N = 2, 4$ ) tapering of the slot depth.

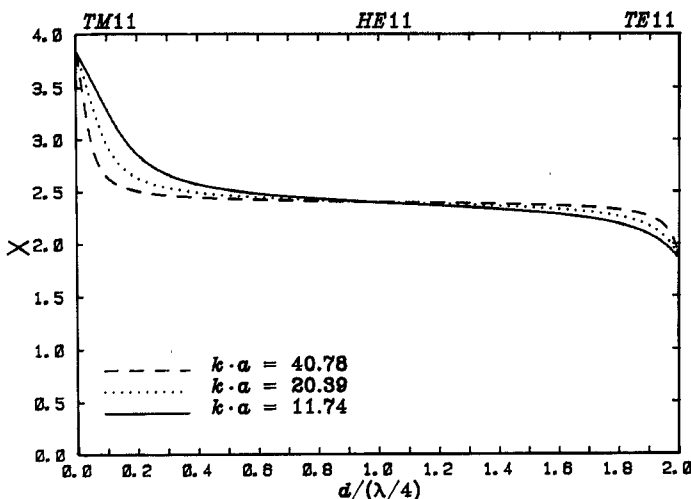


Fig. 8. Radial eigenvalue  $X_{11}$  of the HE<sub>11</sub> hybrid mode versus normalized electrical slot depth  $d/(\lambda/4)$  in circumferentially corrugated waveguides with different  $ka$  values.

TABLE II  
CHARACTERISTIC RESULTS FOR LONG TE<sub>11</sub>-TO-HE<sub>11</sub> MODE CONVERTERS

$f$ [GHz]	28	39	53.2
$D$ [mm]	44.45	35.2	27.79
$ka$	13.05	14.39	15.5
$L_2$ [mm]	386	338	289.8
$N$	4	4	7
$p$ [mm]	2	2	1.4
$w$ [mm]	1	1	0.7
Mode purity [%]	99.6	99.4	99.4
TE <sub>11</sub> [%]	86.6	84.9	86.3
TM <sub>11</sub> [%]	13.0	14.5	13.1
Phase difference [°]	177	183	177
Side-lobe level [dB]	-27	-27	-27
Maximum cross polarization [dB]	-40	-41	-43
Input reflection [dB]	-53	-53	-52
Ohmic losses (Cu) [%]	0.2	0.2	0.3

TABLE III  
THEORETICAL DATA FOR SHORT AND LONG TE<sub>11</sub>-TO-HE<sub>11</sub> MODE CONVERTERS AT  $f = 70$  GHz AND  $D = 27.79$  mm

	Short	Long Type (1)	Long Type (2)
$L$ [mm]	148.4	371	371
$N$	9	9	2
$p$ [mm]	1.4	1.4	1.4
$w$ [mm]	0.7	0.7	0.5
TE <sub>11</sub> [%]	85.8	83.0	82.5
TM <sub>11</sub> [%]	13.4	16.3	17.1
TE <sub>12</sub> [%]	0.002	0.013	0.004
TM <sub>12</sub> [%]	0.3	0.52	0.3
TE <sub>13</sub> [%]	0.0008	0.0001	0.0009
TM <sub>13</sub> [%]	0.2	0.06	0.03
TE <sub>14</sub> [%]	0.00004	0.00008	0.0002
TM <sub>14</sub> [%]	0.1	0.04	0.03
TE <sub>15</sub> [%]	0.0001	0.0002	0.00004
TM <sub>15</sub> [%]	0.06	0.009	0.02
TE <sub>16</sub> [%]	0.000002	0.000007	0.000002
TM <sub>16</sub> [%]	0.07	0.02	0.02
Mode purity [%]	99.2	99.3	99.6
Phase difference TE <sub>11</sub> -TM <sub>11</sub> [°]	184	182	186
Side-lobe level [dB]	-26	-27	-26
Maximum cross polarization [dB]	-33	-36	-32
Input reflection [dB]	-56	-54	-61
Ohmic losses (Cu) [%]	0.2	0.5	0.4

changing slot depth  $d(z)$  [4] satisfies the relation

$$c(d) \cdot (\Delta d / \Delta z) = \kappa_c \quad (9)$$

where the constant  $\kappa_c$  is determined by the requirement that the slot depth reach the desired value at the end of the converter. Increase of the  $ka$  value leads to a more rapid change of the propagation constant of the HE<sub>11</sub> hybrid mode (see Fig. 8) and to unwanted coupling between the TE<sub>11</sub>-HE<sub>11</sub> and TM<sub>11</sub>-EH<sub>12</sub> branches at the converter input.

Some characteristic results for optimized short transducers are listed in Table I and for the corresponding optimized long converters in Table II (computations times for long 110 GHz and 140 GHz transformers are prohibitively long). The optimum length of the short 140 GHz transformer is somewhat smaller than  $0.5\lambda_B$  (very high  $ka$  value).

TABLE I  
CHARACTERISTIC RESULTS FOR SHORT TE<sub>11</sub>-TO-HE<sub>11</sub> MODE CONVERTERS

$f$ [GHz]	28	39	53.2	110	140
$D$ [mm]	44.45	35.2	27.79	17.475	27.79
$ka$	13.05	14.39	15.5	20.15	40.78
$L_1$ [mm]	170	140	120.4	91.8	241.5
$N$	4	4	7	10	40
$p$ [mm]	2	2	1.4	0.9	0.7
$w$ [mm]	1	1	0.7	0.45	0.35
Mode purity [%]	99.4	99.2	99.1	99.3	99.1
TE <sub>11</sub> [%]	87.1	84.7	87.6	86.3	81.3
TM <sub>11</sub> [%]	12.3	14.5	11.5	13.0	17.8
Phase difference [°]	180	182	181	184	186
Side-lobe level [dB]	-27	-26	-26	-26	-24
Maximum cross polarization [dB]	-44	-38	-39	-33	-29
Input reflection [dB]	-57	-53	-50	-54	-62
Ohmic losses (Cu) [%]	0.1	0.2	0.3	0.3	0.5

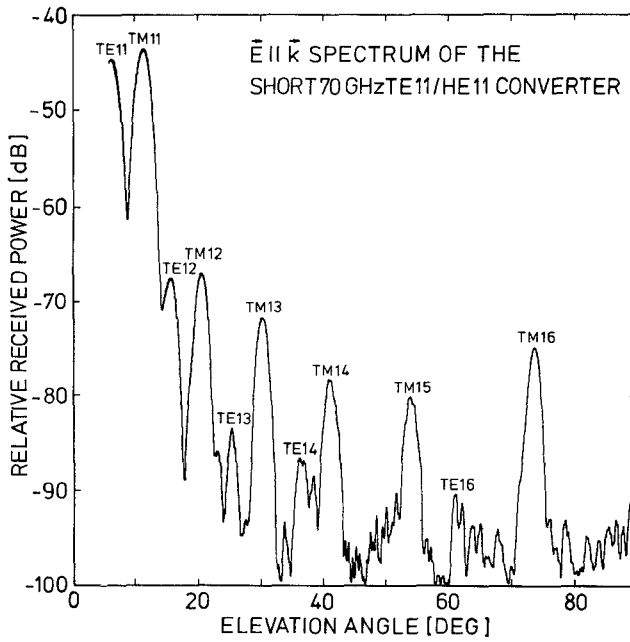


Fig. 9.  $\bar{E} \parallel \bar{k}$  wavenumber spectrum measured at the output of the short 70 GHz  $TE_{11}$  to  $HE_{11}$  mode converter ( $D = 27.79$  mm,  $L_1 = 148.4$  mm).

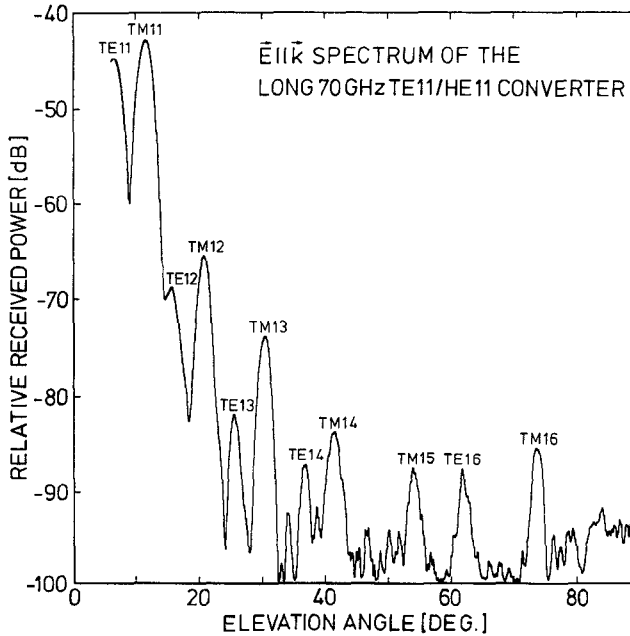


Fig. 10.  $\bar{E} \parallel \bar{k}$  wavenumber spectrum measured at the output of the long 70 GHz  $TE_{11}$  to  $HE_{11}$  mode converter ( $D = 27.79$  mm,  $L_2 = 371.0$  mm).

Theoretical data for different 70 GHz converters ( $D = 27.79$  mm,  $ka = 20.39$ ) including the computed output levels of all propagating  $TE_{1n}$  and  $TM_{1n}$  modes are given in Table III.

The corrugation profile with  $p = 1.4$  mm  $\approx \lambda/3$  and  $w = 0.5$  mm  $\approx \lambda/8$  of the type (2) long converter results in a smoother nonlinear variation of the effective corrugation depth and therefore leads to a low cross-polar level even for  $N = 2$ .

TABLE IV  
RELATIVE  $\bar{E} \parallel \bar{k}$  COUPLING FACTORS OF THE WAVENUMBER SPECTROMETER ( $D = 27.79$  mm) FOR THE MODES  $TE_{1n}$  AND  $TM_{1n}$  ( $n = 1, 2, 3$  AND  $n' = 1, \dots, 6$ ) MEASURED AT 70 GHz (CALIBRATION)

TE Mode	Coupling Factor [dB]	TM Mode	Coupling Factor [dB]
$TE_{11}$	27.0	$TM_{11}$	34.9
$TE_{12}$	14.8	$TM_{12}$	29.1
$TE_{13}$	7.0	$TM_{13}$	27.0
		$TM_{14}$	24.0
		$TM_{15}$	21.9
		$TM_{16}$	23.0

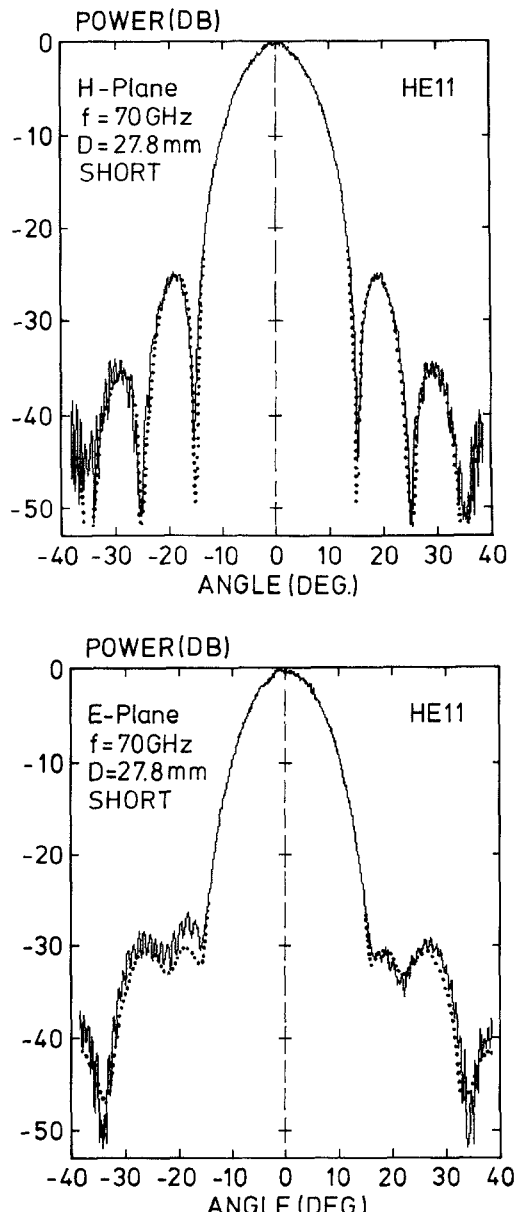


Fig. 11. Measured  $H$ -plane (upper) and  $E$ -plane (lower) far-field radiation patterns of the  $HE_{11}$  mode at the output of the short 70 GHz  $TE_{11}$  to  $HE_{11}$  mode converter ( $D = 27.79$  mm,  $L_1 = 148.4$  mm) generated from a pure  $TE_{11}$  input mode. The theoretical patterns (MAC code) are superimposed (dotted curves). Separation of transmitting and receiving apertures is  $5D^2/\lambda = 920$  mm.

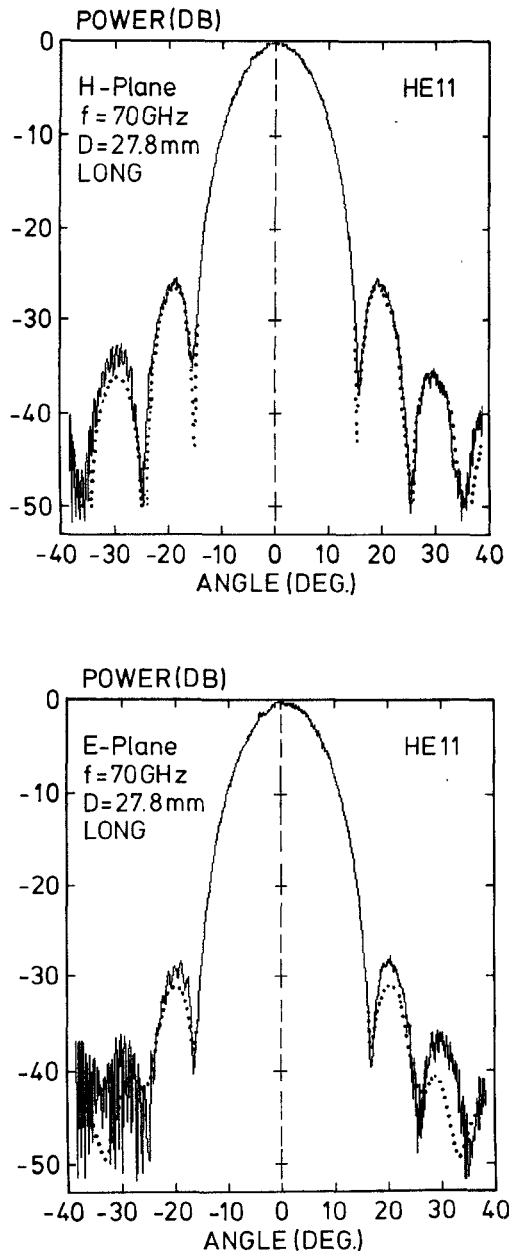


Fig. 12. Measured *H*-plane (upper) and *E*-plane (lower) far-field radiation patterns of the  $HE_{11}$  mode at the output of the long 70 GHz  $TE_{11}$  to  $HE_{11}$  mode converter ( $D = 27.79$  mm,  $L_2 = 371.0$  mm) generated from a pure  $TE_{11}$  input mode. The theoretical patterns (MAC code) are superimposed (dotted curves). Separation of transmitting and receiving apertures is  $5D^2/\lambda = 920$  mm.

## V. EXPERIMENTAL RESULTS

The short and the type (2) long 70 GHz  $TE_{11}$  to  $HE_{11}$  mode converter with  $D = 27.79$  mm ( $ka = 20.39$ ) were fabricated by direct machining on a numerically controlled lathe in the IPF workshop and then tested at low power levels. Millimeter waves at 70 GHz were generated by a 50 mW Gunn oscillator in a fundamental rectangular waveguide (WR-15) and measured with a balanced mixer (LO = 70.8 GHz, IF = 0.8 GHz). The  $TE_{11}$  mode in circular waveguide ( $D = 4.0$  mm) was generated by means of a standard rectangular-to-circular mode transition followed by an optimized nonlinear  $TE_{11}$  up-taper [15] for connecting the small-diameter

circular waveguide to the highly oversized devices under test. The level of unwanted spurious modes ( $TM_{11}$ ,  $TE_{12}$ ) was lower than  $-30$  dB. The  $TE_{1n}$ / $TM_{1n}$  eigenmode content at the output of the  $TE_{11}$  to  $HE_{11}$  mode converters and the corresponding input reflections were measured using a smooth-walled wavenumber spectrometer [16]. The experimental arrangement was terminated by a matched load. Pattern symmetry, side-lobe level, and cross-polarization were determined by computerized measurements of the far-field radiation patterns (copolar *H* and *E* planes and cross-polar  $45^\circ$  plane). The power was received with a small probing horn antenna (low gain) located at distances of about  $5D^2/\lambda$  from the output aperture of the converters. The insertion losses of the  $TE_{11}$  to  $HE_{11}$  transducers were determined by first inserting and then removing two  $TE_{11}$  to  $HE_{11}$  back-to-back converters between two  $TE_{10}^0$  to  $TE_{11}^0$  transitions. A phase deterioration technique (change of waveguide length) was used.

The theoretical design data and the corresponding experimental values are in excellent agreement. Figs. 9 and 10 plot the  $\bar{E}||\bar{k}$  wavenumber spectra (eigenmode content) at the output of the short and long 70 GHz  $TE_{11}$  to  $HE_{11}$  mode converters, respectively. The relative  $\bar{E}||\bar{k}$  coupling factors of the wavenumber spectrometer ( $D = 27.79$  mm) measured at 70 GHz for the modes  $TE_{1n}$  ( $n = 1, 2, 3$ ) and  $TM_{1n}$  ( $n' = 1, \dots, 6$ ) are summarized in Table IV. Both measured spectra are in good agreement with the computed  $TE_{1n}$ / $TM_{1n}$  eigenmode content given in Table III. With the exception of the somewhat increased, but still negligible, amount of higher  $TM_{1n}$  modes ( $n = 3, 4, 5, 6$ ) of the short transducer, the mode purities in both cases are practically identical, the measured insertion losses are  $(0.7 \pm 0.2)\%$ , and the experimentally determined input reflection is lower than  $-50$  dB.

The almost identical *H*-plane and *E*-plane far-field patterns measured at the outputs of the short and long mode transformer are shown in Figs. 11 and 12, respectively. The agreement of the experimental power distributions with the theoretical ones (dotted curves) is very good. The small discrepancies are due to unavoidable mechanical tolerances and measurement errors. The measured maximum cross-polar side-lobe level in the  $45^\circ$  plane is, as predicted, at approximately  $-30$  dB.

## VI. CONCLUSIONS

A theoretical study of  $TE_{11}$  to  $HE_{11}$  mode conversion in highly overmoded, circumferentially corrugated waveguides with different inner diameters is given for various frequencies between 28 and 140 GHz. The corrugation slot depth is gradually tapered from one half to one quarter wavelength.

Computer-aided optimization of corrugation shape, converter length, and nonlinear slot depth variation has been achieved using the modular analysis concept (scattering matrix formalism). The optimum slot-depth profile provides almost constant coupling along the converter between the desired  $TE_{11}$ - $HE_{11}$  mode branch and the unwanted  $TM_{11}$ - $EH_{12}$  mode branch.

Owing to cyclic mode beating and phasing effects, several optimum solutions exist. Relatively short mode transducers with matched converter lengths are feasible. The optimum conversion lengths are  $L_1 \approx 0.5\lambda_B$  (short converter) and  $L_2 \approx 1.2\lambda_B$  (long converter), where  $\lambda_B$  is the beat wavelength of the  $TE_{11}$  and  $TM_{11}$  modes in the corresponding smooth-

walled circular waveguide. The predicted performances of short and long mode transducers are practically identical.

Experimental results taken at 70 GHz (I.D. = 27.79 mm) are in excellent agreement with the theoretically predicted performance data. In all cases the  $HE_{11}$  output mode purity is 99% to 99.5% with good pattern symmetry and low side-lobe level of  $\leq -25$  dB. The peak cross-polarization does not exceed -29 dB and the input reflection turns out to be below -50 dB.

The advantage offered by the modular analysis concept (MAC) over the surface impedance description is that it allows an optimization of the converter performance and a tolerance analysis taking accurately into account all relevant geometrical parameters. The MAC concept is capable of predicting both the return loss and the  $TE_{1n}/TM_{1n}$  eigen-mode content (amplitudes and phases) at the output of  $TE_{11}$  to  $HE_{11}$  mode transducers within the measurement accuracy.

#### ACKNOWLEDGMENT

The authors are indebted to Dr. E. Kühn from the Forschungsinstitut der Deutschen Bundespost in Darmstadt for many valuable suggestions and for his permission to use the MAC scattering matrix code. We acknowledge with gratitude many helpful discussions with W. Henle, W. Kasparek, G. Müller, and J. Prettner from the Institut für Plasmaforschung (IPF). Thanks are also due to H. Hermann, G. Röpke, G. Lang, and D. Wimmer from the technical staff of the IPF for the mechanical design and precise machining of the corrugated mode converters.

#### REFERENCES

- [1] J. L. Doane, "Mode converters for generating the  $HE_{11}$  (Gaussian like) mode from  $TE_{01}$  in a circular waveguide," *Int. J. Electron.*, vol. 53, pp. 573-585, Dec. 1982.
- [2] M. Thumm *et al.*, "Generation of the Gaussian-like  $HE_{11}$  mode from gyrotron  $TE_{0n}$  mode mixtures at 70 GHz," *Int. J. Infrared and Millimeter Waves*, vol. 6, pp. 459-470, June 1985.
- [3] P. J. B. Clarricoats and A. D. Oliver, *Corrugated Horns for Microwave Antennas* (IEE Electromagnetic Waves Series 18). London: Peter Peregrinus, 1984.
- [4] N. P. Kerzhentseva, "Conversion of wave modes in a waveguide with smoothly varying impedance of the walls," *Radio Eng. Electron. Phys.*, vol. 16, pp. 24-31, Jan. 1971.
- [5] C. Dragone, "Reflection, transmission, and mode conversion in a corrugated feed," *Bell Syst. Tech. J.*, vol. 56, pp. 835-867, July-Aug. 1977; "Characteristics of a broadband microwave corrugated feed: A comparison between theory and experiment," *Bell Syst. Tech. J.*, vol. 56, pp. 869-888, July-Aug. 1977.
- [6] G. L. James, "Analysis and design of  $TE_{11}$ -to- $HE_{11}$  corrugated cylindrical waveguide mode converters," *IEEE Trans. Microwave Theory Tech.*, vol. MTT-29, pp. 1059-1066, Oct. 1981.
- [7] G. L. James, " $TE_{11}$ -to- $HE_{11}$  mode converters for small angle corrugated horns," *IEEE Trans. Antennas Propagat.*, vol. AP-30, pp. 1057-1062, Nov. 1982.
- [8] B. MacA. Thomas, G. L. James, and K. J. Greene, "Design of wide-band corrugated conical horns for cassegrain antennas," *IEEE Trans. Antennas Propagat.*, vol. AP-34, pp. 750-757, June 1986.
- [9] E. Kühn and V. Hombach, "Computer-aided analysis of corrugated horns with axial or ring-loaded radial slots," in *Proc. 3rd Int. Conf. Antennas and Propagation (ICAP 83)*, 1983, pp. 127-131.
- [10] A. D. Oliver and J. Xiang, "Wide angle corrugated horns analysed using spherical mode-matching," *Proc. Inst. Elec. Eng.*, pt. H, vol. 135, pp. 34-40, Feb. 1988.
- [11] M. Thumm, "Computer-aided analysis and design of corrugated  $TE_{11}$  to  $HE_{11}$  mode converters in highly overmoded waveguides," *Int. J. Infrared and Millimeter Waves*, vol. 6, pp. 577-597, July 1985.
- [12] M. Thumm, A. Jacobs, and M. Sorolla, "Short high-power  $TE_{11}$ - $HE_{11}$  mode converters in highly overmoded corrugated waveguides," in *Conf. Dig. 14th Int. Conf. Infrared Millimeter Waves (Würzburg)*, 1989, pp. 152-153.
- [13] I. V. Lindell and A. H. Sihvola, "Dielectrically loaded corrugated waveguide: Variational analysis of a nonstandard eigenproblem," *IEEE Trans. Microwave Theory Tech.*, vol. MTT-31, pp. 520-526, July 1983.
- [14] C. Dragone, "Attenuation and radiation characteristics of the  $HE_{11}$ -mode," *IEEE Trans. Microwave Theory Tech.*, vol. MTT-28, pp. 704-710, July 1980.
- [15] M. Thumm *et al.*, "Very high power mm-wave components in oversized waveguides," *Microwave J.*, vol. 29, pp. 103-121, Nov. 1986.
- [16] W. Kasparek and G. A. Müller, "The wavenumber spectrometer—An alternative to the directional coupler for multimode analysis in oversized waveguides," *Int. J. Electron.*, vol. 64, pp. 5-20, Jan. 1988.

✉

**Manfred Thumm** was born in Magdeburg, Germany, on August 5, 1943. He received the Dipl. Phys. and Dr. rer. nat. degrees in physics from University of Tübingen, Tübingen, Germany, in 1972 and 1976, respectively. At the University of Tübingen he was involved in the investigation of spin-dependent nuclear forces in inelastic neutron scattering. From 1972 to 1975 he was a Doctoral Fellow of the Studienstiftung des deutschen Volkes.



In 1976 he joined the Institute for Plasma Research in the Electrical Engineering Department of the University of Stuttgart, Stuttgart, Germany, where he worked on RF production and RF heating of toroidal pinch plasmas for thermonuclear fusion research. From 1982 to May 1990 his research activities were mainly devoted to electromagnetic theory in the areas of component development for the transmission of very high power millimeter waves through overmoded waveguides and of antenna structures for RF plasma heating with microwaves. In June 1990 he became a full professor at the Institute for Very High Frequency Technology and Electronics of the University of Karlsruhe, Karlsruhe, Germany, and Head of the Gyrotron Development and Microwave Technology Division in the Institute for Technical Physics of the Nuclear Research Center (Kernforschungszentrum) at Karlsruhe.

✉



**Annemarie Jacobs** was born in Tübingen, Germany, on May 31, 1963. She received the Dipl. Ing. degree in electrical engineering from University of Stuttgart, Stuttgart, Germany, in October 1987.

At the Institute for Plasma Research of the University of Stuttgart her research deals with the development of transmission and mode conversion systems in overmoded waveguides for high-power millimeter-wave tubes such as gyrotrons.



**Mario Sorolla Ayza** (S'85-M'88) was born in Vinaròs, Spain, on October 19, 1958. He received the telecommunication engineer degree from the Politechnic University of Barcelona, Barcelona, Spain, in 1984.

He then worked on low-noise down-converters for satellite TV at the firm TAGRA, S.A. (near Barcelona, Spain) and at the same time taught circuit theory at the Politechnic University of Barcelona (center of Vilanova). In 1986 he joined the Association Euratom-

Ciemat in Madrid (Spain), where he was involved in the design of very high power millimeter waveguide components for plasma heating in thermonuclear controlled fusion. During this time, he was guest scientist at the Institute for Plasma Research of the University of Stuttgart, Stuttgart, Germany, for 18 months. There he completed designs of high-power waveguide components. He is now with Mier Comunicaciones, S.A. (near Barcelona) as a design engineer working on MMIC and solid-state power amplifiers. Mr. Sorolla expects to present his Ph.D. dissertation, on very high power oversized waveguide components, at the Politechnic University of Madrid in 1991.